Catalytic steam reforming of volatiles release via pyrolysis of wood sawdust for hydrogen-rich gas production on Fe-Zn/Al_2O_3 nanocatalysts

Fangyuan Chen[a,c], Chunfei Wu[b,d*], Lisha Dong[a], Fangzhu Jin[a], Paul T. Williams[b*], Jun Huang[a*]

[a] *School of Chemical and Bimolecular Engineering, the University of Sydney, Australia, NSW 2037 (Tel: +61 2 9351 7483; Email: jun.huang@sydney.edu.au)*

[b] *Energy Research Institute, University of Leeds, Leeds LS2 9JT, UK (Tel: +44 113 3432504; Email: p.t.williams@leeds.ac.uk)*

[c] *School of Environmental Science & Engineering, Kunming university of Science & Technology, Kunming 650038, P. R. China*

[d] *School of Engineering, University of Hull, Hull HU6 7RX, UK (Tel: +44 1482466464; Email: c.wu@hull.ac.uk)*

Abstract:

Thermo-chemical processing of biomass is a promising alternative to produce renewable hydrogen as a clean fuel or renewable syngas for a sustainable chemical industry. However, the fast deactivation of catalysts due to coke formation and sintering limits the application of catalytic thermo-chemical processing in the emerging bio-refining industry. In this research, Fe-Zn/Al_2O_3 nanocatalysts have been prepared for the production of hydrogen through pyrolysis catalytic reforming of wood sawdust. Through characterization, it was found that Fe and Zn were well distributed on the surface with a narrow particle size. During the reactions, the yield of hydrogen increased with the increase of Zn content, as Zn is an efficient metal promoter for enhancing the performance of the Fe active site in the reaction. The 20% Fe/Al_2O_3 catalyst with Zn/Al ratio of 1:1 showed the best performance in the process in relation to the hydrogen production and resistance to coke formation on the surface of the reacted catalyst. All the catalysts showed ultra-high stability during the process and nearly no sintering were observed on the used catalysts. Therefore, the nanocatalysts prepared from natural-abundant and low-cost metals in this work have promising catalytic properties (high metal dispersion and stability) to produce H_2-rich syngas with optimal H_2/CO ratio from the thermo-chemical process of biomass.

Keywords: biomass; catalyst; gasification; hydrogen; syngas; nano-catalysts

1. Introduction

Hydrogen is one of the few long-term sustainable clean energy carriers as it emitting only water vapour as a by-product during the combustion and oxidation process [1-3]. However, hydrogen production can be environmentally friendly only if the resource used to extract hydrogen is carbon neutral [4]. Biomass is one of the most abundant forms of carbon neutral resources, and biomass gasification is a promising alternative to produce renewable hydrogen as a clean fuel or renewable syngas (CO_2, CO, H_2) for a sustainable chemical industry [5-9]. Of all the thermo-chemical processes, however, biomass gasification still suffers from lower hydrogen production and higher tar formation compared to the process using fossil fuels. Recently, biomass catalytic gasification has been shown to greatly increase hydrogen yield and decreased tar formation. Dolomite, CeO_2/SiO_2 supported Ni, Pt, Pd, Ru and alkaline metal oxides have been reported to be effective in tar reduction and conversion efficiency [5]. However, one significant challenge for catalytic gasification is the fast deactivation of catalysts due to coke formation and sintering, which limits the application of catalytic gasification in the emerging bio-refining industry [10-12]. Therefore, developing highly stable catalysts with satisfactory catalytic properties are highly desired for biomass gasification.

It was widely accepted that the catalyst stability and activity are based on its physical structure and chemical composition. For supported metal catalysts in biomass gasification, many synthesis methods have been reported to control the size of nanoparticles and increase the dispersion of active metals to enhance the activity of catalysts. Moreover, the activity and stability can be further improved after using various supports and promoters to generate the support-metal interaction on catalysts. For example, the mixture of MgO or CaO with alumina supports could strongly enhance the interaction between supports and surface atoms of metal particles, which could strongly stabilize the metal particles to block their sintering on supports and also enhance the metal activity due to the electron transfer between support and surface [13-

17]. Recently, introducing ZnO to the supports was reported to achieve high catalytic performance in methanol reforming and methyl-benzoate hydrogenation [18-20]. Lu et al. found that the catalyst of ZnO supported on γ- Al_2O_3 has a higher activity than ZnO or ZnO supported on SiO_2, β-Zeolite, and MCM-41 [20]. Interestingly, it was observed that ZnO could cover the surface acidity of alumina support and further enhance the reducibility of supported metal particles [21-24]. Not only for better metal dispersion and size control [25], the strong interaction between ZnO and metal particles could also prevent sintering and catalytic poisoning under working conditions [26-27].

For the potential industrial application, the catalysts based on expensive noble metals such as Pt and Pd were replaced by the naturally abundant and low-cost transition metals such as Ni and Fe [28-32]. Unlike popular Ni catalysts in the catalytic gasification and reforming, there are only limited researches about Fe catalysts in biomass gasification due to its relatively low catalytic activity. However, Fe was believed to be catalytically active for reducing heavy hydrocarbons in the gas product during the thermo-chemical process [33-39]. It has also been adopted as a stable and active catalyst for the water-gas shift reaction (WGSR) [40]. In this study, therefore, Fe catalysts on ZnO/Al_2O_3 supports have been prepared by a co-precipitation method. The effect of Zn for the catalytic behavior of the catalyst，especially activity and carbon deposition, were investigated for the pyrolysis catalytic steam reforming of wood sawdust using a two-stage reaction system.

2. Experimental

2.1 Materials

Wood sawdust was used in this work as raw biomass with a size less than 0.2 mm. The physical properties of the wood sawdust are reported in our previous work [3]. The catalysts were prepared by a co-precipitation method with and initial Fe-loading mole ratio of 20 mol%. Fe $(NO_3)_3 \cdot 6H_2O$(≥99%), $Zn(NO_3)_3 \cdot 6H_2O$(≥99%), $Al_2(NO_3)_3 \cdot 9H_2O$(≥99%) were purchased from Sigma-Aldrich. Precursors with the

desired Fe-ZnO/Al_2O_3 ratios were prepared by dissolving a certain amount of metal salts in deionized water. After the precipitation, the suspension was aged under agitation for an hour and then filtered under vacuum. The filter cake obtained was rinsed with deionzed water several times followed by drying at 80 °C over night. The solid products were calcined at 800 °C for 4h with a heating rate of 1 min^{-1} in static air.

2.2 Pyrolysis/catalytic steam reforming process

Pyrolysis/ catalytic steam reforming was carried out with a fixed bed, two-stage reaction system was shown in Figure 1. There are two stages in the reaction system. Pyrolysis of biomass was performed in the first reaction stage, the derived pyrolysis vapours were catalytic steam reformed in the second stage. The two stages were externally electrically heated with separated temperature controllers. During the experiment, N_2 (80 $mlmin^{-1}$) was used as carrier gas. 0.5 g of biomass was placed inside a crucible and held in the first pyrolysis reactor. 0.25 g of sand/catalyst was placed in the second reactor. The temperature of the second reactor was initially heated to the set point (800 °C). Then the first reactor was heated to the pyrolysis temperature (500 °C) at a heating rate of 40 min^{-1} and kept at that temperature for 30 min. Water for steam reaction was injected between the two reactors with an injection rate of 0.05g min^{-1} when the temperature of the pyrolysis reactor reached 150 °C, while carrier gas N_2 was used during the whole experiment. The products from the pyrolysis/catalytic steam reforming were cooled using air and dry ice to collect the condensed liquid. It is noted that tar compounds in the liquid product were not analyzed, since gas and hydrogen product were mainly investigated in this work. The non-condensed gases were collected using a Tedlar^{TM} gas bag, and further analyzed off-line using packed column gas chromatograph (GC). It was allowed to collect the non-condensed gases to ensure complete reaction in ca. 20 min. The amounts of injected water and the condensed liquid were calculated by weighting the syringe and condensers before and after the experiment, respectively. Experiments were repeated to ensure the reliability of the results.

2.3 Gas analysis and catalyst characterization

Non-condensed gases collected in the Tedlar™ gas bag were analysed off-line by GC. H_2, CO and N_2 were analyzed with a Varian 3380 GC on a 60-80 mesh molecular sieve column with argon carrier gas, whilst CO_2 was analyzed by another Varian 3380 GC on a Hysep 80-100 mesh column with argon carrier gas. C_1-C_4 hydrocarbons were analyzed using a Varian 3380 gas chromatograph with a flame ionistion detector, with an 80-100 mesh Hysep column and nitrogen carrier gas. Quantities of gas products including H_2, CO, CO_2, CH_4 and C_2-C_4 hydrocarbons were obtained using carrier gas (N_2) as internal standard. During the discussions in this work, gas composition was presented excluding N_2.

BET surface area of the fresh catalyst was analysed by N_2 adsorption and desorption isotherms on a Quantachrome Autosorb-1. X-Ray Diffraction (XRD) analysis was carried out on the fresh catalysts by using a SIEMENS D5000 in the range of 10°-70° with a scanning step of 0.02° using Cu Kα radiation (0.1542 nm wavelength). A high resolution scanning electron microscope (SEM) (LEO 1530) coupled to an energy dispersive X-ray spectroscope (EDXS) system was used to investigate the surface morphology and the element distributions of the reacted catalysts.

Temperature programmed reduction (TPR) was used to characterize the fresh catalysts using a Stanton-Redcroft thermogravimetric analyzer (TGA). During the TPR analysis, the fresh catalyst was heated at 20 ˚C min^{-1} to 150 ˚C and held for 30 min, then heated at 10 ˚C min^{-1} to 900 ˚C in an atmosphere of gas mixture containing 5% H_2 and 95%N_2 (50 ml min^{-1}).

Temperature-programmed oxidation (TPO) of the reacted catalysts was carried out using a Stanton-Redcroft thermogravimetric analyzers (TGA and DTG) to determine the properties of the coked carbons deposited on the reacted catalysts. About 10 mg of the reacted catalyst was heated in an atmosphere of air at 15 min^{-1} to a final temperature of 800 °C, with a dwell time of 10 min. The coke amount was calculated from the weight loss of sample (300-500 °C) divided by the original sample weight.

3. Results and discussion

3.1 Characteristics of Fe-Zn/Al_2O_3 catalysts

The theoretical metal composition, particle size and BET surface area of the catalysts are shown in Table 1. The surface areas of Fe-Zn/Al_2O_3 catalysts prepared by the co-precipitation method greatly decreased from 72.8 to 11.6 m^2g^{-1} with the increase of Zn/Al ratio from 1:4 to 1:1 in the catalyst.

XRD patterns of Fe-Zn/Al_2O_3 catalysts were used to identify the species present in the catalysts as shown in Figure 2. $FeAl_2O_4$ and $Zn(AlFe)O_4$ species were observed mainly at 31 and 36^o for the XRD spectra of the catalyst with Zn/Al ratio of 1:1. However, Fe_2O_3 (mainly at 24 and 33 ^{o}) and $ZnAl_2O_4$ (mainly at 37^o) are dominant species on all other Fe-Zn/Al_2O_3 catalysts. It was observed that the peak intensity of both Fe_2O_3 and $ZnAl_2O_4$ species increased with the increasing of the Zn/Al ratio from 1:4 to 1:2. Further increasing the Zn/Al ratio to 1:1, the spinels, i.e., $FeAl_2O_4$ and $Zn(AlFe)O_4$, were dominant on the catalysts. It indicates that the formation of ferric oxide or ferric spinels in the catalysts was related to the Zn/Al ratio: ferric oxide was mainly generated on the catalysts with the Zn/Al ratio lower than 1:2; high Zn/Al ratio of 1:1 promoted the formation of ferric spinels. Zn reacted preferentially with Al to form $ZnAl_2O_4$ spinel when the Zn was at a lower amount in the catalysts. However, when the amount of Zn increased to a certain level, i.e., the ratio of Zn/Al of around 1 in this case, Zn could react with both Fe and Al to form $FeAl_2O_4$ and $Zn(AlFe)O_4$.

SEM images did not clearly show these spinels on the surface of the Fe-Zn/Al_2O_3catalysts as shown in Figure 3. With the increase of the Zn content, the surfaces of the catalysts tended to be clearer and less fine grained particles were observed.

Therefore, H_2-TPR has been used to further determine the surface species on Fe-Zn/Al_2O_3 catalysts and their reducibility. As shown in Figure 4, TPR curves for the catalysts with the Zn/Al ratios from 1:4 to 1:2 were characterized by three main

reduction peaks: the first centered at around 400 °C for the reduction of ferric oxide to FeO or Fe; the second peak of FeO reduced at 600 °C; and the third one for the reduction of Fe contained spinels at 900°C [42]. With the increase of the Zn/Al ratio of 1:1, the third peak gradually shifted from 900 °C to 800 °C, showing the increased reducibility of the compound. Spinels were mainly formed on the catalyst as confirmed by the dominant peak at a reduction temperature at 800 °C, which was also confirmed by the above XRD investigation. Only a very small amount of ferric oxide particles were located on the surface as indicated by the very weak reduction peak at 400 °C on the TPR curve and the SEM imagine of this catalyst. Zinc aluminates were non-reduced in the whole range of studied temperatures.

3.2 Experimental tests on Fe-Zn/Al_2O_3 catalysts

Gasification of the sawdust was carried out on Fe-Zn/Al_2O_3 catalysts under a water stream at 800 °C and the results are summarized in Table 2. From the calculation based on the mass balance, it was noted that the yields of both total gas and hydrogen were obviously increased with the addition of catalysts during thermo-chemical process. For the catalysts with ferric oxide and spinels as the main surface species (the Zn/Al ratio of the catalysts from 1:4 to 1:2), total gas yields were obtained between ca. 33 to 40 wt.% with hydrogen yields from 2.4 to 7 mmol H_2/gsample, respectively. While for the catalyst with only spinels as the main component, i.e., the Zn/Al ratios of 1:1, both gas and hydrogen yields were further increased up to 50 wt.% and 9.7 mmolH_2/g sample, respectively. Though the Fe-Zn/Al_2O_3 catalyst with a Zn/Al ratio of 1:1 exhibits the lowest BET surface area (6 times lower than the catalysts with a Zn/Al ratio of 1:4) in these catalysts, it contributed the highest activity in terms of hydrogen production, indicating that the BET surface area is not the key factor for the estimation of catalytic activity in this research. Therefore, the catalytic performance on the prepared catalysts was mainly depended on their surface active sites. Catalysts with only Fe contained spinels on surface offered the highest catalytic activity and hydrogen production during the biomass thermo-chemical processing. However, the existence of ferric oxide or FeO

on the surface would drop down the reactivity of catalysts even both species were easily reduced to active Fe for the process.

Obviously, introducing Zn into the catalysts promoted the formation of spinels and enhanced reaction process. The change of gas composition with various Zn/Al ratio in catalysts has been summarized in Figure 5. The hydrogen fraction in gas kept almost the same level at ca. 35 Vol.% with the increasing of the ratio of Zn/Al from 1:4 to 1:2. Also, with the increase of Zn/Al ratio from 1:4 to 1:2, the CO fraction in the individual product gas increased from around 28 to 32 Vol.%, and the CO_2 fraction decreased from 23 to 19 Vol.%. Meanwhile, the fraction of hydrocarbon gas (CH_4 and C_2-C_4) was similar on three catalysts. Therefore, the dry or steam reforming of small hydrocarbons has not been influenced by the Zn/Al ratios. The WGSR of CO and water was slightly decreased with the increase of Zn. These catalysts containing both ferric oxide/FeO and Fe spinels performed similarly for the hydrogen production.

The hydrogen and CO_2 fractions were increased to 40 and 24 Vol.% with the strongly decreased CO fraction to 24 Vol.% and slightly decreased hydrocarbon fractions when the Zn/Al ratio increased to 1:1. Obviously, the spinel only catalyst could promote the hydrogen production mainly based on the WGSR as CO amount decreased proportionally with the increase of CO_2 amount. Also, slightly improved dry reforming of hydrocarbons contributed to additional hydrogen production. The obtained gas product derived from the Fe-Zn/Al_2O_3 (1:1) catalyst has an optimal H_2/CO ratio (ca. 2), which is favored for the hydrocarbon synthesis process such as Fischer-Tropsch.

3.3 Coke formation

The above research reported that the Fe spinel dominated catalyst had much better catalytic performance compared to catalysts containing both ferric oxide/FeO and Fe spinels. Normally, better catalytic performance always relates to the heavy coke formation on catalysts, which is a significant challenge for the biomass thermo-chemical and causes a fast catalyst deactivation. In this research, the amount of coke on

various catalyst has been determined via temperature programmed oxidation (TPO) as shown in Figure 6. The coke amount was subtracted by the weight loss of the normal TPO results for Fe particles produced during thermo-chemical process. Only one type of carbon formed on the surface of the catalyst, with an oxidation peak at around 400°C. It might be assigned to amorphous carbon, which is relatively easy to be removed during regeneration compared with graphite carbons.

Detailed quantitation of the coke on the catalysts was calculated based on TPO results and is shown in Figure 7. For the catalysts (Zn/Al ratio from 1:4 to 1:2) offering similar surface active species and catalytic performances, the amount of coke decreased from 5.5 to 2.5 wt.% with the increase of the Zn content. Even no change for the surface active sites, adding Zn could strongly reduce the coke formation. The possible reason was reported previously that Zn could cover the surface acid sites and limit the coke deposition on the surface [8-10]. On Fe spinel only catalyst (Zn/Al ratio of 1:1), the coke amount was only ca. 0.5 wt.%, which is very low compared to regular catalysts used for biomass gasification [43]. Clearly, spinel only catalyst not only offers highest catalytic activity, but also has significant resistance to coke formation.

It was reported that Fe active sites could be dispersed atomically in the spinel structure to improve tar decomposition during the gasification [36-38]. This kind of high dispersion of Fe on spinel catalyst could overcome its shortage of the much lower surface area compared to a mixture of oxides and contribute the higher gas production and hydrogen yield during the thermo-chemical process. It should be noted that the spinel structure is thermally stable during the reaction and resistant to sintering as reported by previous research [44-46]. In this research SEM was used to show the surface morphology of all the reacted catalysts. As shown in Figure 8, SEM did not show the obvious difference of the catalysts' surface compared with the surface of the fresh catalysts (Figure 3). It indicates no sintering on catalyst surface during gasification and the high stability of the prepared catalysts.

4. Conclusions

In this work, the pyrolysis catalytic reforming of wood sawdust was performed on nano Fe-Zn/Al_2O_3 catalysts. During the thermo-chemical process, the yield of hydrogen was increasing up to maximum with the ratio of Zn/Al from 1:4 to 1:1. Obviously, Zn is an efficient metal promoter for enhancing the performance of Fe active site in the reaction. Adding Zn could sharply reduce the surface area of catalysts. The higher conversion rates on these catalysts were mainly depended on the highly dispersed Fe active sites in Fe spinels. Catalysts with dominated Fe spinel on surface offered the highest catalytic activity and hydrogen production during the thermo-chemical process based on the enhanced WGSR and hydrocarbon dry reforming. However, the existence of ferric oxide or FeO on the surface would drop down the reactivity of catalysts even both species were easily reduced to active Fe for the process. Introducing even small amount of Zn could strongly improve the stability of catalysts. As shown in SEM imagines, all catalysts showed ultra-high stability during the process and nearly no sintering has been observed on the used catalysts. Spinel only catalyst also showed higher resistance for coke formation, only 0.5 wt.% coke was produced during the thermo-chemical conversion process and the coke was hard to be observed on the surface of catalyst by SEM. It was demonstrated that Zn promoted Fe nanocatalysts prepared from natural-abundant and low-cost metals using the simple method have the targeting catalytic properties and stability for biomass thermo-chemical processing.

Acknowledgements

This work was supported by the International Exchange Scheme from the Royal Society (IE110273), UK, and the Early Career Research Scheme from the University of Sydney.

References

[1] V.A. Goltsov, T.N. Veziroglu, L.F. Goltsova. Hydrogen civilization of the future—A new conception of the IAHE. Int J Hydro Energy 2006; 31:153-159.

[2] M. Ni, D.Y.C. Leung, M.K.H. Leung, K. Sumathy. An overview of hydrogen production from biomass. Fuel Processing Technol 2006; 87:461-472.

[3] C. Wu, L. Wang, P.T. Williams, J. Shi, J. Huang. Hydrogen production from biomass gasification with Ni/MCM-41 catalysts: Influence of Ni content. Appl Catal B 2011;108–109:6-13.

[4] L. Wang, C.L. Weller, D.D. Jones, M.A. Hanna. Contemporary issues in thermal gasification of biomass and its application to electricity and fuel production. Biomass Bioenergy 2008;32: 573-581.

[5] D. Sutton, B. Kelleher, J.R.H. Ross. Review of literature on catalysts for biomass gasification. Fuel Processing Technol 2001; 73; 155-173.

[6] P.M. Mortensen, J.D. Grunwaldt, P.A. Jensen, K.G. Knudsen, A.D. Jensen. A review of catalytic upgrading of bio-oil to engine fuels. Appl Catal A 2011; 407: 1-19.

[7] A.K. Olaleye, K.J. Adedayo, C. Wu, M.A. Nahil, M. Wang, P.T. Williams. Experimental study, dynamic modelling, validation and analysis of hydrogen production from biomass pyrolysis/gasification of biomass in a two-stage fixed bed reaction system. Fuel 2014;137:364-374.

[8] A. Tanksale, J.N. Beltramini, G.M. Lu. A review of catalytic hydrogen production processes from biomass. Renewable and Sustainable Energy Reviews 2010; 14 :166-182.

[9] P. Parthasarathy, K.S. Narayanan. Hydrogen production from steam gasification of biomass: Influence of process parameters on hydrogen yield – A review. Renewable Energy 2014; 66: 570-579.

[10] C. Font Palma. Modelling of tar formation and evolution for biomass gasification: A review. Appl Energy 2013; 111: 129-141.

[11] Y. Shen, K. Yoshikawa. Recent progresses in catalytic tar elimination during biomass gasification or pyrolysis—A review. Renewable Sustainable Energy Rev 2013;

21: 371-392.

[12] F.L. Chan, A. Tanksale. Review of recent developments in Ni-based catalysts for biomass gasification. Renewable Sustainable Energy Rev 2014;38: 428-438.

[13] Y.-G. Chen, K. Tomishige, K. Yokoyama, K. Fujimoto. Catalytic Performance and Catalyst Structure of Nickel–Magnesia Catalysts for CO2 Reforming of Methane. J Catal 1999;184 :479-490.

[14] K. Tomishige, Y.-g. Chen, K. Fujimoto. Studies on Carbon Deposition in CO2Reforming of CH4over Nickel–Magnesia Solid Solution Catalysts. J Catal 1999;181: 91-103.

[15] A.A. Lemonidou, M.A. Goula, I.A. Vasalos. Carbon dioxide reforming of methane over nickel calcium aluminate catalysts – effect of preparation method. Catal Today 1998; 46:175-183.

[16] C.K.S. Choong, L. Huang, Z. Zhong, J. Lin, L. Hong, L. Chen. Effect of calcium addition on catalytic ethanol steam reforming of Ni/Al2O3: II. Acidity/basicity, water adsorption and catalytic activity. Appl Catal A 2011;407:155-162.

[17] J.A.C. Dias, J.M. Assaf. Influence of calcium content in Ni/CaO/γ-Al2O3 catalysts for CO2-reforming of methane. Catal Today 2003;85:59-68.

[18] J. Agrell, M. Boutonnet, J.L.G. Fierro. Production of hydrogen from methanol over binary Cu/ZnO catalysts: Part II. Catalytic activity and reaction pathways. Appl Catal A 2003;253: 213-223.

[19] M. Turco, G. Bagnasco, U. Costantino, F. Marmottini, T. Montanari, G. Ramis, et al.. Production of hydrogen from oxidative steam reforming of methanol: II. Catalytic activity and reaction mechanism on Cu/ZnO/Al2O3 hydrotalcite-derived catalysts. J Catal 2004; 228:56-65.

[20] W. Lu, G. Lu, X. Liu, Y. Guo, J. Wang, Y. Guo. Effects of support and modifiers on catalytic performance of zinc oxide for hydrogenation of methyl benzoate to benzaldehyde. Mater Chem Phys 2003; 82:120-127.

[21] M.N. Barroso, M.F. Gomez, L.A. Arrúa, M.C. Abello. Hydrogen production by ethanol reforming over NiZnAl catalysts. Appl Catal A 2006;304:116-123.

[22] J. Chen, Y. Qiao, Y. Li. Promoting effects of doping ZnO into coprecipitated Ni-Al2O3 catalyst on methane decomposition to hydrogen and carbon nanofibers. Appl Catal A 2008;337:148-154.

[23] J. Chen, Y. Qiao, Y. Li. Modification of Ni state to promote the stability of Ni–Al2O3 catalyst in methane decomposition to produce hydrogen and carbon nanofibers. J Solid State Chem 2012;191 :107-113.

[24] R. Buitrago-Sierra, J. Ruiz-Martínez, J.C. Serrano-Ruiz, F. Rodríguez-Reinoso, A. Sepúlveda-Escribano. Ethanol steam reforming on Ni/Al2O3 catalysts: Effect of the addition of Zn and Pt. J Colloid Interface Sci 2012;383: 148-154.

[25] T. Shishido, Y. Yamamoto, H. Morioka, K. Takehira. Production of hydrogen from methanol over Cu/ZnO and Cu/ZnO/Al2O3 catalysts prepared by homogeneous precipitation: Steam reforming and oxidative steam reforming. J Mol Catal A 2007; 268:185-194.

[26] M. Yang, Y. Men, S. Li, G. Chen. Hydrogen production by steam reforming of dimethyl ether over ZnO–Al2O3 bi-functional catalyst. Int J Hydro Energy 2012; 37:8360-8369.

[27] B.V. Farahani, F.H. Rajabi, M. Bahmani, M. Ghelichkhani, S. Sahebdelfar. Influence of precipitation conditions on precursor particle size distribution and activity of Cu/ZnO methanol synthesis catalyst. Appl Catal A 2014; 482 :237-244.

[28] M. Ni, D.Y.C. Leung, M.K.H. Leung, A review on reforming bio-ethanol for hydrogen production. Int J Hydro Energy 2007;32: 3238-3247.

[29] A.E. Castro Luna, M.E. Iriarte. Carbon dioxide reforming of methane over a metal modified Ni-Al2O3 catalyst. Appl Catal A 2008; 343:10-15.

[30] L. Chen, C.K.S. Choong, Z. Zhong, L. Huang, Z. Wang, J. Lin. Support and alloy effects on activity and product selectivity for ethanol steam reforming over supported nickel cobalt catalysts. Int J Hydro Energy 2012;37:16321-16332.

[31] T.V. Reshetenko, L.B. Avdeeva, A.A. Khassin, G.N. Kustova, V.A. Ushakov, E.M. Moroz, et al.. Coprecipitated iron-containing catalysts (Fe-Al_2O_3, Fe-Co-Al_2O_3, Fe-Ni-Al_2O_3) for methane decomposition at moderate temperatures: I. Genesis of calcined

and reduced catalysts. Appl Catal A 2004;268: 127-138.

[32] T.V. Reshetenko, L.B. Avdeeva, V.A. Ushakov, E.M. Moroz, A.N. Shmakov, V.V. Kriventsov, et al.. Coprecipitated iron-containing catalysts (Fe-Al2O3, Fe-Co-Al2O3, Fe-Ni-Al2O3) for methane decomposition at moderate temperatures: Part II. Evolution of the catalysts in reaction, Appl Catal A 2004; 270:87-99.

[33] L. Wang, D. Li, M. Koike, S. Koso, Y. Nakagawa, Y. Xu, K. Tomishige. Catalytic performance and characterization of Ni-Fe catalysts for the steam reforming of tar from biomass pyrolysis to synthesis gas. Appl Catal A 2011;392: 248-255.

[34] T. Nordgreen, T. Liliedahl, K. Sjöström. Metallic iron as a tar breakdown catalyst related to atmospheric fluidised bed gasification of biomass. Fuel 2006;85: 689-694.

[35] D. Świerczyński, S. Libs, C. Courson, A. Kiennemann. Steam reforming of tar from a biomass thermo-chemical process over Ni/olivine catalyst using toluene as a model compound. Appl Catal B 2007;74 :211-222.

[36] L. Devi, K.J. Ptasinski, F.J.J.G. Janssen. Pretreated olivine as tar removal catalyst for biomass gasifiers: investigation using naphthalene as model biomass tar. Fuel Processing Technol 2005;86 :707-730.

[37] L. Devi, K.J. Ptasinski, F.J.J.G. Janssen. A review of the primary measures for tar elimination in biomass thermo-chemical processes. Biomass Bioenergy 2003;24:125-140.

[38] J.N. Kuhn, Z. Zhao, L.G. Felix, R.B. Slimane, C.W. Choi, U.S. Ozkan. Olivine catalysts for methane- and tar-steam reforming. Appl Catal B 2008; 81: 14-26.

[39] G. Duman, T. Watanabe, M.A. Uddin, J. Yanik. Steam gasification of safflower seed cake and catalytic tar decomposition over ceria modified iron oxide catalysts. Fuel Processing Technol 2014;126: 276-283.

[40] A. Venugopal, M.S. Scurrell. Low temperature reductive pretreatment of Au/Fe2O3 catalysts, TPR/TPO studies and behaviour in the water–gas shift reaction. Appl Catal A 2004;258:241-249.

[41] C. Wu, P.T. Williams. Pyrolysis–gasification of plastics, mixed plastics and real-world plastic waste with and without Ni–Mg–Al catalyst. Fuel 2010;89:3022-3032.

[42] M. Liang, W. Kang, K. Xie. Comparison of reduction behavior of Fe_2O_3, ZnO and $ZnFe_2O_4$ by TPR technique. J Natural Gas Chem 2009; 18: 110-113.

[43] J. Nishikawa, T. Miyazawa, K. Nakamura et al. Promoting effect of Pt addition to $Ni/CeO_2/Al_2O_3$ catalyst for steam gasification of biomass. Catal Commu 2008; 9: 195-201

[44] S. Hull, J. Trawczyński. Steam reforming of ethanol on zinc containing catalysts with spinel structure. Int J Hydro Energy 2014;39:4259-4265.

[45] H. Muroyama, R. Nakase, T. Matsui, K. Eguchi. Ethanol steam reforming over Ni-based spinel oxide, Int J Hydro Energy 2010;35:1575-1581.

[46] J. Sehested, J.A.P. Gelten, I.N. Remediakis, H. Bengaard, J.K. Nørskov. Sintering of nickel steam-reforming catalysts: effects of temperature and steam and hydrogen pressures. J Catal 2004; 223:432-443.

Table 1 Composition, size and surface areas of the Fe-Zn/Al_2O_3 catalysts

Sample	Molar Ratio (Zn/Al)	Theoretical Metal Composition (wt.%)[a]			Particle size (nm)[b]				BET surface area (m^2g^{-1})
		Fe	Zn	Al_2O_3	$FeAl_2O_4$	$ZnFe_2O_4$	α-Fe_2O_3	$ZnAl_2O_4$	
Fe-Zn/Al_2O_3	1:1-	19.46	45.1	35.5	-	-	-	-	11.6
Fe-Zn/Al_2O_3	1:2	20.0	31.3	48.7	-	-	46.0	20.3	28.0
Fe-Zn/Al_2O_3	1:3	20.4	23.8	55.8	-	-	46.3	12.8	52.8
Fe-Zn/Al_2O_3l	1:4	20.6	19.3	60.1	-	-	-	12.0	72.8

[a] The theoretical metal composition was calculated via the equation M=M/(Fe+Zn+Al_2O_3), where M represents Fe or Zn

[b] Particle size obtained from XRD data calculated from Scherrer's formula

Table 2 Mass balance of the catalytic reforming of vapours derived from pyrolysis of sawdust on Fe-Zn/Al_2O_3 catalysts

Catalyst bed	Sand	Fe-Zn/Al_2O_3			
		1:1	1:2	1:3	1:4
Gas/Biomass (wt.%)	33.01	48.68	43.36	39.80	39.61
Residue/Biomass (wt.%)	38.81	38.75	37.50	36.25	37.50
Mass balance (wt.%)	103.3	99.52	104.64	99.88	98.62
H_2 yield (mmol H_2/g)	2.40	9.65	7.25	6.79	6.59

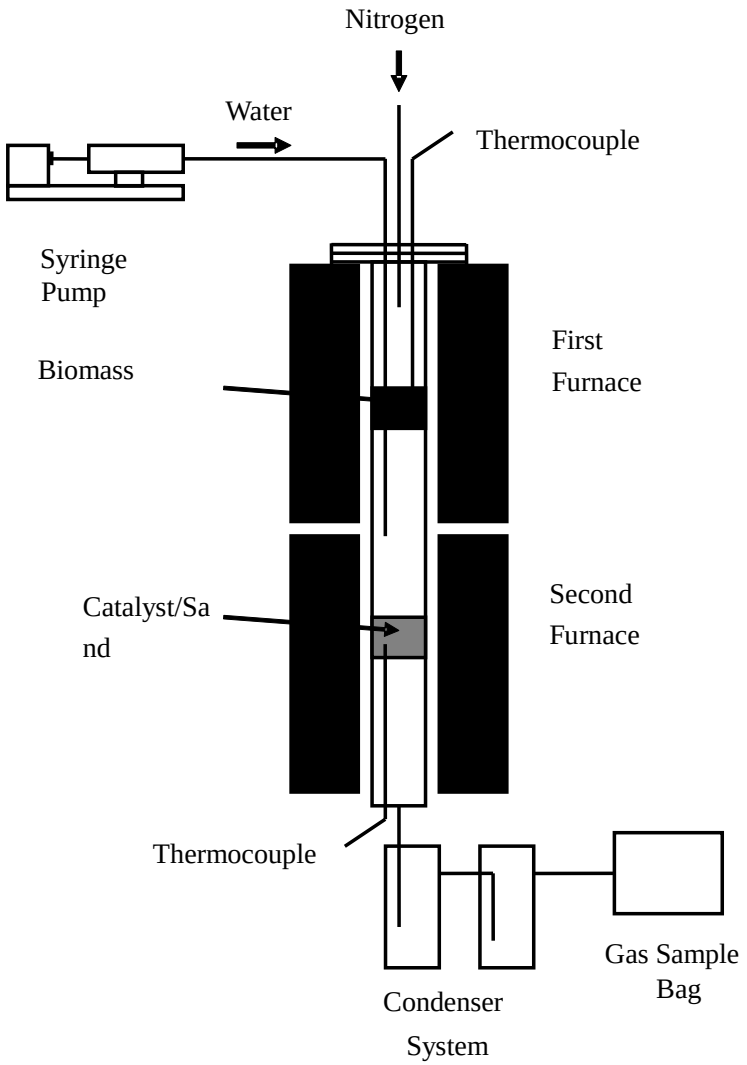

Figure Schematic diagram of the reaction system

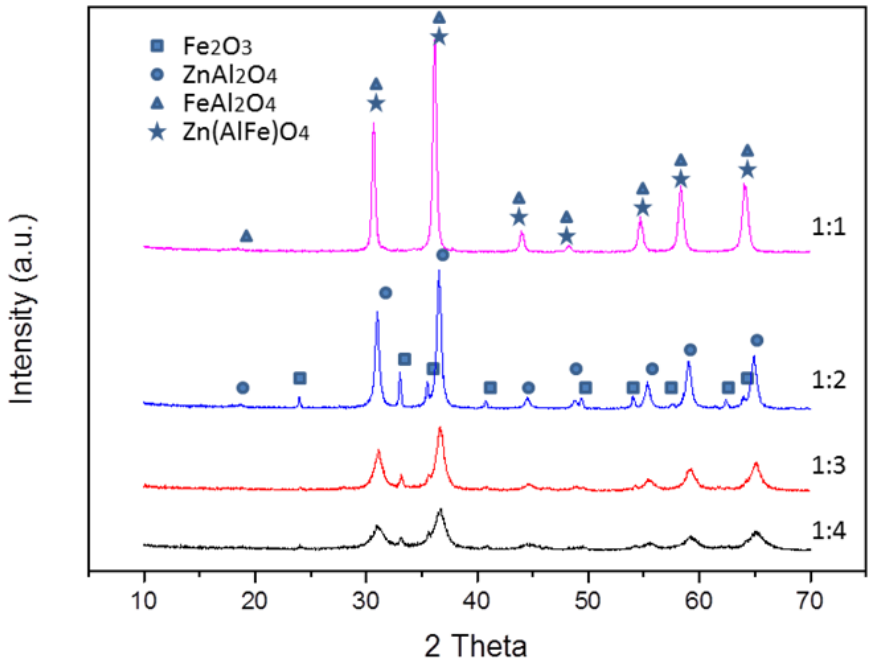

Figure 2 XRD patterns of the fresh Fe-Zn/Al_2O_3 catalysts with Zn/Al ratios of 1:1, 1:2, 1:3 and 1:4, respectively

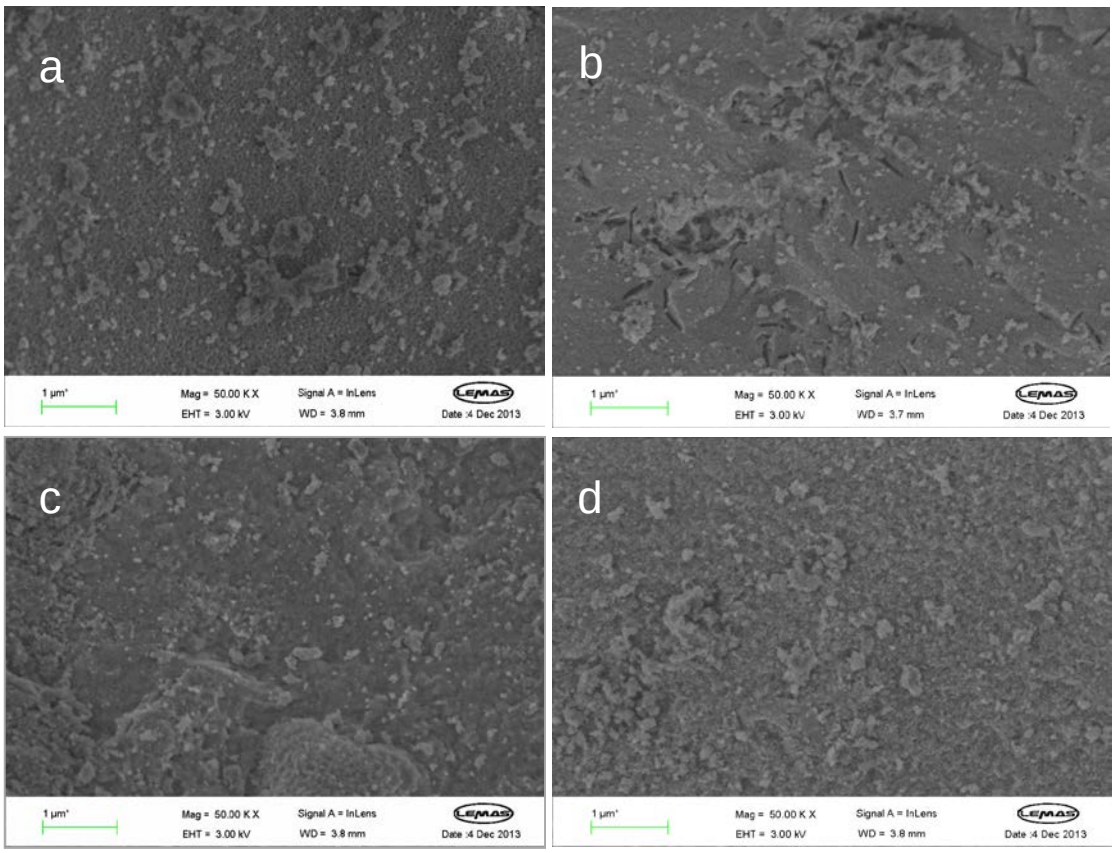

Figure 3 SEM imagines of the fresh Fe-Zn/Al_2O_3 catalysts: (a) Zn/Al=1:1; (b) Zn/Al=1:2; (c) Zn/Al=1:3; (d) Zn/Al=1:4

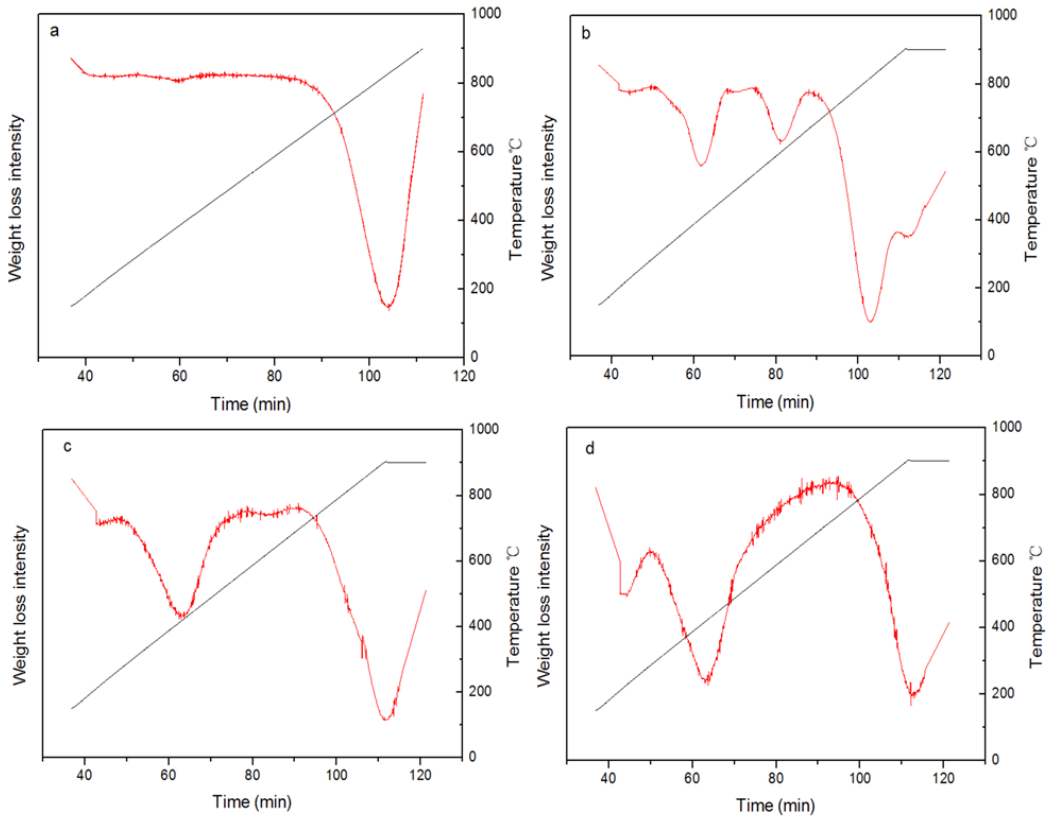

Figure 4 TPR results of the Fe-Zn/Al_2O_3 catalysts: (a) Zn/Al=1:1; (b) Zn/Al=1:2; (c) Zn/Al=1:3; (d) Zn/Al=1:4

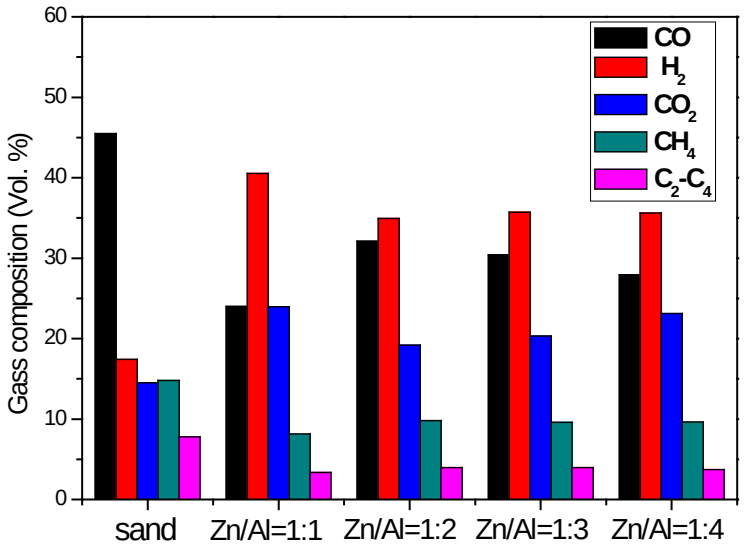

Figure 5 Gas compositions and fractions from biomass thermo-chemical processing on the Fe-Zn/Al_2O_3 catalysts

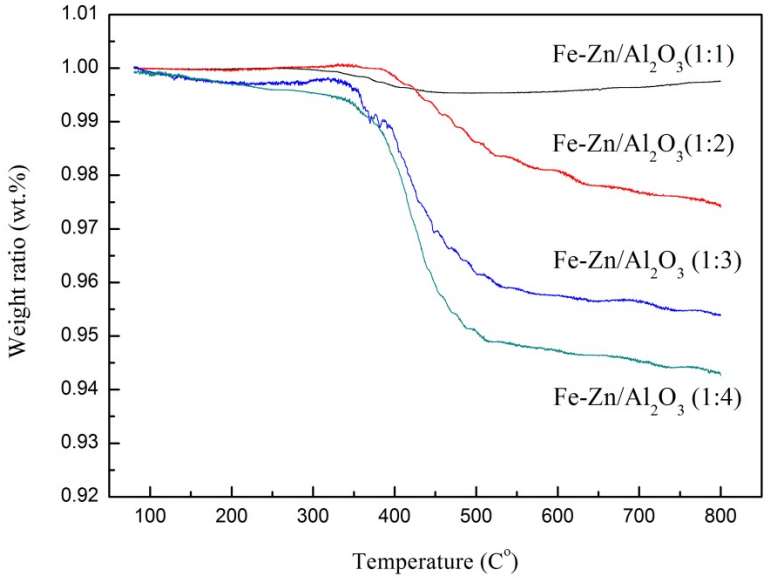

Figure 6 TPO analyses of the reacted Fe-Zn/Al_2O_3 catalysts

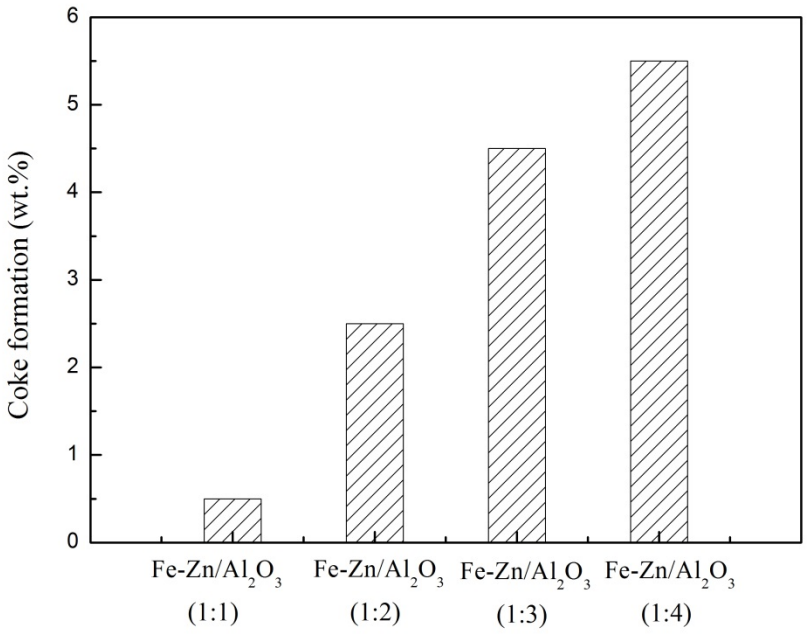

Figure 7 Weight ratios of coke to the catalyst for the reacted Fe-Zn/Al_2O_3 catalysts.

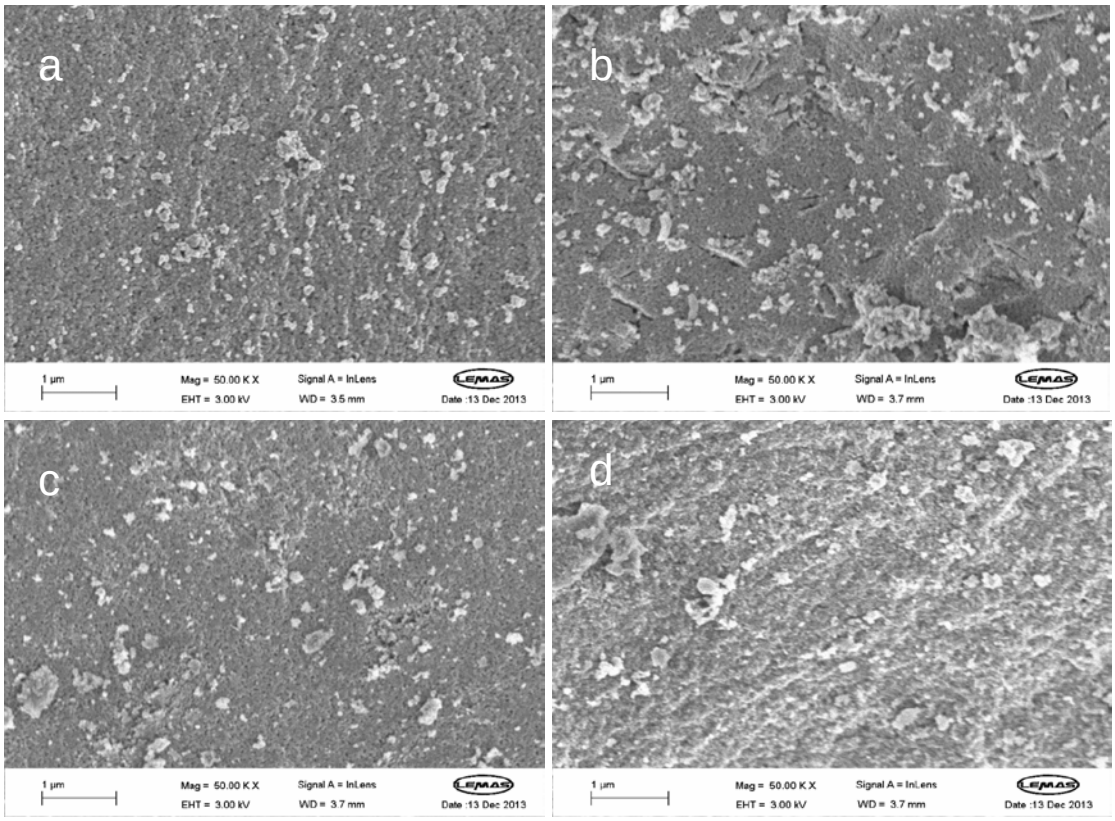

Figure 8 SEM imagines of the reacted Fe-Zn/Al_2O_3catalysts: (a) Zn/Al=1:1; (b) Zn/Al=1:2; (c) Zn/Al=1:3; (d) Zn/Al=1:4